Journal of Power Sources 195 (2010) 2844–2850

Contents lists available at ScienceDirect

Journal of Power Sources

journal homepage: www.elsevier.com/locate/jpowsour

Synthesis and performance of carbon-coated $Li_3V_2(PO_4)_3$ cathode materials by a low temperature solid-state reaction

Lijuan Wang, Xuechou Zhou, Yonglang Guo*

College of Chemistry and Chemical Engineering, Fuzhou University, Fuzhou 350108, PR China

ARTICLE INFO

Article history:
Received 9 June 2009
Received in revised form 9 September 2009
Accepted 13 November 2009
Available online 9 December 2009

Keywords:
Lithium vanadium phosphate
Carbon coat
Cathode material
Lithium ion batteries
Solid-state reaction

ABSTRACT

The carbon-coated monoclinic $Li_3V_2(PO_4)_3$ (LVP) cathode materials can be synthesized by a low temperature solid-state reaction route. The influences of different heat treatments on the LVP have been investigated using X-ray diffraction (XRD), scanning electron microscopy (SEM) and electrochemical methods. In the range of 3.0–4.3 V, both LVP/C electrodes present good rate capability and excellent cyclic performance. It is found that the sample (LVP1/C) prepared by the two-step heat treatment with pre-sintering at 350 °C delivers the initial discharge capacity of 99.8 mAh g^{-1} at 10 C charge–discharge rate and still retains 95.8 mAh g^{-1} after 300 cycles. For the sample (LVP2/C) synthesized by the one-step heat treatment, 95.9 and 90.0 mAh g^{-1} are obtained in the 1st and 300th cycles at 10 C rate, respectively. Our results based on the XRD patterns and the SEM images suggest that the good rate capability and cyclic performance may be owing to the pure phases, small particles, large specific surface areas and residual carbon. In the range of 3.0–4.8 V, compared with the LVP2/C, the LVP1/C also exhibits better performance.

1. Introduction

Recently, monoclinic $Li_3V_2(PO_4)_3$ (LVP) has been extensively researched as a promising cathode material proposed for lithium ion batteries [1–19]. In the LVP, all three Li^+ ions are mobile. Two Li^+ ions can be extracted and inserted reversibly in the range of 3.0–4.3 V based on the V^{3+}/V^{4+} redox couple. When charged to 4.8 V, all three Li^+ ions can be fully extracted from the lattice to yield a theoretical capacity of 197 mAh g^{-1},which is the highest reported for any phosphate [1,2].

To date, the synthesis of the LVP has been a subject matter of immense interest and a number of techniques have been employed such as conventional high temperature solid-state reaction [20–22], low temperature solid-state route [23], sol–gel method [17,24], rheological phase reaction synthesis [10], hydrothermal synthesis [12], chemical reduction and lithiation method [25], and other solution routes [8,9,14,26]. For the conventional high temperature solid-state process, however, high calcination temperature and long sintering time are needed, which results in a large particle size and aggregation of the final product. In addition, it is difficult to mix the raw materials homogeneously by the solid-state process and impurity phases can also be found in the final product. In a word, the electrochemical performance of the product obtained via a high temperature solid-state route will be adversely influenced by the factors above. For a solution route, although a high reaction temperature is not required and high capacities can be delivered, long reaction time and some additional processes, such as stirring and heating, are also needed. Hence, a simple and convenient route to synthesize LVP with high electrochemical performance is highly desired. It is clearly observed from the previous literatures reported that the preparation conditions including reaction temperature and time, the physicochemical properties of the final product involved in structure, purity, morphology, and electrochemical performance are influenced by the precursor or starting materials [23]. Thus, a proper choice of raw materials is important to the fabrication of cathode materials with high performance for lithium ion batteries.

In this work, a route to prepare the LVP/C with high electrochemical performance from $LiOH{\cdot}H_2O$, NH_4VO_3, $NH_4H_2PO_4$, $H_2C_2O_4{\cdot}2H_2O$ and $C_6H_{12}O_6{\cdot}H_2O$ at a relatively low temperature and the effects of different heat treatments on the structures and physicochemical properties of the LVP/C composite materials are studied.

2. Experimental

2.1. Synthesis of $Li_3V_2(PO_4)_3/C$

The LVP/C composite materials were synthesized by a low temperature solid-state route. The precursors were prepared as

* Corresponding author at: Applied Chemistry, College of Chemistry and Chemical Engineering, Fuzhou University, Fuzhou 350108, PR China. Tel.: +86 591 8807 3608; fax: +86 591 8807 3608.
E-mail address: yguo@fzu.edu.cn (Y. Guo).

0378-7753/$ – see front matter © 2009 Elsevier B.V. All rights reserved.
doi:10.1016/j.jpowsour.2009.11.056

follows: stoichiometric $LiOH{\cdot}H_2O$, NH_4VO_3, $NH_4H_2PO_4$ and an appropriate amount of $H_2C_2O_4{\cdot}2H_2O$ were added into a little deionized water and then mixed by ball-milling for 4 h. After the mixture was dried at 60 °C in a vacuum oven, a certain amount of $C_6H_{12}O_6{\cdot}H_2O$ and the dry mixture above were dispersed into ethanol and ball milled another 1 h. Then, as-prepared precursors were heat-treated according to two different methods as follows:

(1) The precursor was pressed into pieces and heated at 350 °C for 2 h, then heated to 700 °C and held at this temperature for 6 h in a temperature-controlled tube furnace under N_2 atmosphere to obtain the LVP1/C material.
(2) The precursor was pressed into pieces and sintered at 700 °C for 6 h under N_2 atmosphere to prepare the LVP2/C sample.

The carbon content was determined by dissolving the synthesized LVP/C products into hydrochloric acid with the help of the ultrasonic wave and weighing the remainders after 5 days. And the content of both samples is about 11.5 wt.%.

2.2. Physical characterization and electrochemical measurements

Structural and crystallographic analysis of the products synthesized were taken from the powder X-ray diffraction data obtained using a Rigaku D/max III X-ray Diffractometer with Cu Kα radiation (λ = 1.54059 Å). The diffraction patterns were recorded in the 2θ range from 10° to 80° with a scanning speed 2° min^{-1}. The cell parameters of the materials were calculated by the Whole Pattern Fitting (WPF) programme. The morphologies and particle sizes of the samples were observed by an XL30ESEM (Philips) scanning electron microscope (SEM).

The electrochemical tests were performed using CR2025 coin-type cells. For the fabrication of the electrodes, 85 wt.% active materials were mixed with 10 wt.% carbon black and 5 wt.% polyvinylidene difluoride (PVDF) in an appropriate amount of N-methyl-2-pyrrolidine until slurry was obtained. Then it was pasted onto the aluminum current collectors and the electrodes were dried at 120 °C in vacuum for 12 h. The active material loading was in the range of 4.0–4.5 mg cm^{-2}. The assembly of the test cells was carried out in a glove box filled with high purity argon. The lithium metal foil was served as the counter electrode, Celgard2320 as the separator, and 1 M $LiPF_6$ dissolved in a mixture of ethylene carbonate (EC) and dimethyl carbonate (DMC) with the volume ratio of 1:1 as the electrolyte. The charge–discharge measurements were conducted on a Land Battery Test system in the ranges of 3.0–4.3 V and 3.0–4.8 V, respectively. Cyclic voltammograms (CVs) and the electrochemical impedance spectroscopies (EIS) were performed by a CHI 660C electrochemical workstation. The CV tests were done between 3.0 and 4.3 V at a scanning rate of 0.1 mV s^{-1}, and the EIS were measured by applying an *ac* voltage of 5 mV in the frequency range of 10 mHz to 100 kHz. All tests were carried out at room temperature.

3. Results and discussion

3.1. Synthesis

Low temperature solid-state route possesses lower calcination temperature than the high temperature solid-state method. In the present work, a low temperature solid-state reaction route using a carbothermal reduction (CTR) of vanadium with high valence [1,21,22] has been introduced to fabricate the LVP/C composite materials selecting $LiOH{\cdot}H_2O$, NH_4VO_3, $NH_4H_2PO_4$, $H_2C_2O_4{\cdot}2H_2O$ and $C_6H_{12}O_6{\cdot}H_2O$ as starting materials. The key to the route is the choice of the raw materials, that is to say, some materials with crystal water are required. A little crystal water from the raw materials is released under ball milling and a thin water film is formed on the surface of the reactants, based on which well-mixed precursor will be obtained, the low temperature reaction will be highly promoted and additional solvent will also be greatly reduced.

Besides, glucose is employed as carbon sources for reduction and coating. And oxalic acid acts not only as a chelating agent and a reduction agent [27] but also as a carbon source and an inhibitor because a large quantity of gas can be released owing to the decomposition of the oxalate. The growth and agglomeration of the particles will be inhibited to a certain extent due to the gas released. It is can be seen from the SEM results below that the particle size of the LVP/C is small and the agglomeration of the particles is not too severe. It is confirmed that the structure and physicochemical properties of the final product are greatly affected by different carbon sources [11,28]. Since oxalic acid and glucose may provide carbon in an inert atmosphere, and it is possible that the two carbon sources are complementary, the properties of the products from the two carbon sources are better compared with those of the samples from the single carbon source [27].

3.2. Sample characterization

The XRD patterns of the LVP1/C and LVP2/C composite materials are presented in Fig. 1, in which all diffraction lines can be attributed to the single-phase $Li_3V_2(PO_4)_3$ and indexed as monoclinic structure with a space group ($P2_1/n$). Additionally, no other secondary phases such as V_2O_3, VPO_4 and Li_3PO_4 are detected from the XRD patterns. The results are in good agreement with the previous reports by Huang et al. [1], Saidi et al. [5], Yin et al. [6]. It is clear that the XRD patterns of both samples are similar, implying that the monoclinic structure of the products based on different heat treatments has no change. The sharp diffraction peaks and strong diffraction intensities are demonstrated, that is to say, good crystallinities are achieved for the two samples, which is advantageous to their electrochemical properties. Moreover, no additional diffraction peak related-carbon is detected in the XRD patterns, which is undoubted as the residual carbon is amorphous or the coating carbon layer on the LVP particles is too thin [29]. The cell parameters of the LVP1/C and LVP2/C composite materials are listed in Table 1. The cell parameters are similar to those in previous reports [1,6] and vary slightly for the two samples. It indicates that different heat treatments do not have significant effects on the cell parameters of the products.

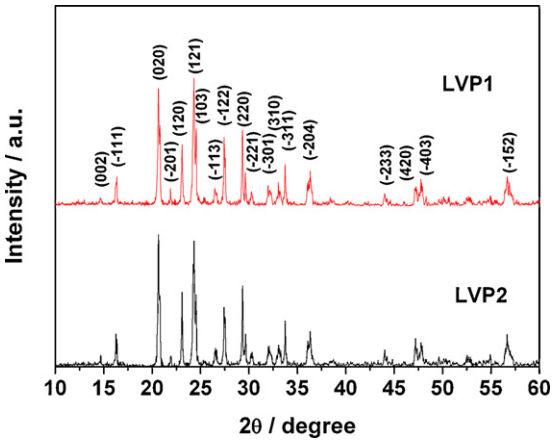

Fig. 1. X-ray diffraction patterns of LVP1/C and LVP2/C composite materials.

Table 1
Cell parameters of the $Li_3V_2(PO_4)_3$ samples.

Samples	a (Å)	b (Å)	c (Å)	β (°)	V (Å^3)
LVP1	8.618(8)	8.601(3)	12.042(9)	90.47(7)	892.8(0)
LVP2	8.616(1)	8.601(9)	12.044(9)	90.47(8)	892.7(0)

The SEM images were used to identify the morphologies and measure the particle sizes of the synthesized materials, as shown in Fig. 2. For the two composite materials, their surface is rough, and some small particles bound on the surface of the LVP are observed, which can be considered as scattered carbon particles. The stabilization of V^{3+} can be favored, the diffusion of Li^+ ion will be facilitated and the composite materials with superior conductivity are formed owing to the residual carbon. Furthermore, for high specific surface area carbon acts as a nucleation site for material growth, suppressing extensive grain growth in the product from morphological research [21], relatively small particles are got for the composite materials of LVP1/C and LVP2/C. Most particles for the LVP1/C and LVP2/C are between 0.5 and 1 μm and are smaller than the ones from traditional high temperature solid-state reaction [30]. Then, large specific surface area of particles and uniform particle size are presented for the two samples, which will play important roles on the cyclic performance of the products [23]. In addition, notable agglomeration is not observed as to the samples, which may be related to the decomposition of the oxalate to produce a great deal of gas and the existence of the carbon layer. Nevertheless, a great difference is observed between the LVP1/C and LVP2/C. Many LVP1 particles are embedded in a continuous carbon network, and some particles with subspherical shape are adhered to the surface of that, based on which good electronic contact among the LVP1 particles will be obtained. For the LVP2, some particles coated with carbon are separate and are not too regular in the shape. The large space between LVP2 particles will increase the electrochemical reaction resistance. The abundance of grain-boundary will lead to poor connection of the LVP2 particles, which is attributed to the high contact resistance. The high electrochemical reaction resistance and contact resistance may be responsible for the low initial discharge specific capacities of the LVP2/C.

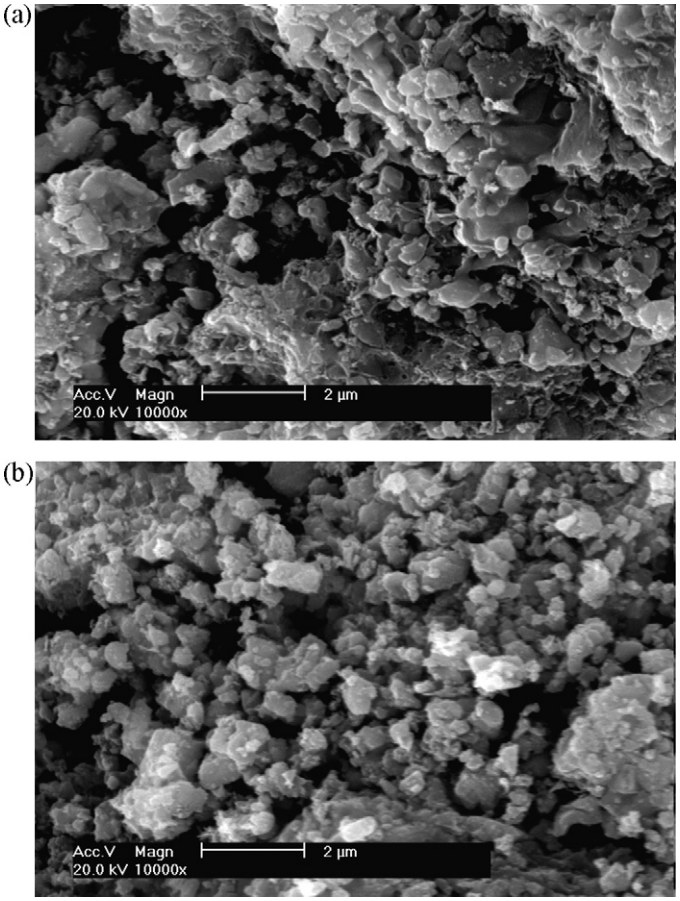

Fig. 2. SEM images of (a) LVP1/C and (b) LVP2/C.

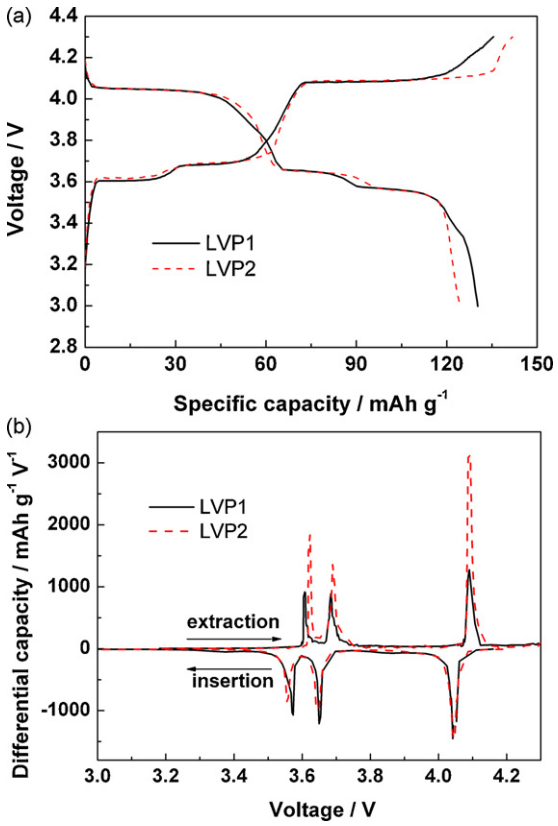

Fig. 3. (a) Initial charge–discharge profiles of LVP1/C and LVP2/C at 0.2 C rate in the range of 3.0–4.3 V and (b) their corresponding differential capacity plots.

3.3. Electrochemical performance

3.3.1. Galvanostatic electrochemical measurements

The initial charge–discharge profiles of the carbon-coated LVP1 and LVP2 electrodes at 0.2 C rate in the range of 3.0–4.3 V and their corresponding differential capacity plots are shown in Fig. 3(a) and (b), respectively. As can be seen, there are three charge plateaus and the corresponding three discharge ones on the curves, which is characteristic of the electrochemical reaction between two complicated phase transition processes [2,6,7,31] and corresponds to three compositional regions of $Li_{3-x}V_2(PO_4)_3$, that is, $x = 0.0$–0.5, 0.5–1.0 and 1.0–2.0. It is noted that both cells exhibit three charge plateaus around 3.61, 3.69 and 4.08 V and corresponding three discharge plateaus around 3.58, 3.65 and 4.05 V. The potential differences between each couple of charge and corresponding discharge plateaus are less than 0.05 V, which manifests that the transport of electrons and ions is easy in the carbon-coated materials. However, it can be seen that the different heat treatments have some effects on the discharge capacity. As shown in Fig. 3(a), the LVP1/C has a longer discharge plateau than the LVP2/C and their initial discharge capacities are 130.4 and 124.4 mAh g^{-1} at 0.2 C rate, respectively. It is in good agreement with the SEM result. The fea-

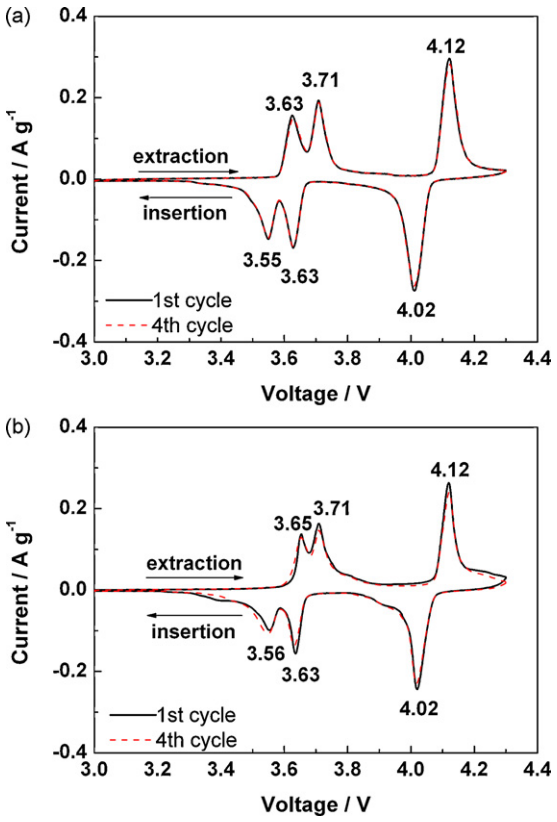

Fig. 4. Cyclic voltammograms for the 1st and 4th cycles of (a) LVP1/C and (b) LVP2/C electrodes at a rate of 0.1 mV s^{-1} in the range of 3.0–4.3 V.

tures in the voltage profiles of the two samples are better depicted in the differential capacity plots.

3.3.2. Cyclic voltammetry (CV)

To further understand the charge–discharge behavior of the LVP1/C and LVP2/C electrodes, the CV curves of the 1st and 4th cycles have been recorded at a scanning rate of 0.1 mV s^{-1} in the range of 3.0–4.3 V and the results are shown in Fig. 4. There are three anodic peaks and three corresponding cathodic ones on the curves for both cells. The three anodic peaks are located around 3.64, 3.71 and 4.12 V, and the cathodic ones about 3.55, 3.63 and 4.02 V, which is in good line with the charge–discharge profiles depicted in Fig. 3(a). The first two anodic peaks correspond to the extraction of the first Li^+ ion with two steps, as the $Li_{2.5}V_2(PO_4)_3$ phase appears in the oxidation process [7], while the second Li^+ ion is removed via a single step corresponding to the third anodic peak. In addition, the reinsertion of the first two Li^+ ion is also associated with the V^{3+}/V^{4+} redox couple.

For the LVP1/C and LVP2/C, similar CV plots are presented, suggesting that different heat treatments have no effects on the structures, the regime for the phase transition and the anodic and cathodic couples during the process of the Li^+ extraction and reinsertion, which is in accordance with the XRD results and charge–discharge measurements. The well-defined peaks and good symmetry of the CV plots confirm the excellent reversibility of the Li^+ extraction and insertion reactions for the LVP/C composite materials.

3.3.3. Rate capability and cyclic performance

It is well known that the rate capability is very important if commercially viable systems are to be developed [22]. In our experiment, both carbon-coated LVP1 and LVP2 exhibit good rate performance. The initial charge–discharge profiles of the two samples between 3.0 and 4.3 V at 3 and 10 C rates are compared in Fig. 5(a). It is observed that there are three charge plateaus and corresponding discharge ones on the curves, which is in agreement with the results of the CV. As shown in Fig. 5(a), for the same charge–discharge rate, the LVP1 electrode presents larger reversible discharge capacity than the LVP2 electrode. When the current density is increased from 3 to 10 C, the initial discharge specific capacity decreases from 103.9 to 99.8 mAh g^{-1} for the LVP1, and from 99.9 to 95.9 mAh g^{-1} for the LVP2. Therefore, the different heat treatments still give some effects on the initial discharge specific capacities of the LVP1 and LVP2 at high rates. Nevertheless, it is apparent that the two products show unexceptionable rate performance. It is possible that it is related to the existence of carbon on the surfaces of the LVP1 and LVP2 particles, which improves the electronic conductivity of the two electrodes.

The voltage–capacity curves of the two samples in the 1st, 300th and 600th cycles for 3 C rate and in the 1st, 150th and 300th cycles for 10 C rate are shown in Fig. 5(b)–(e). It is seen that the charge–discharge plateaus of the products become short with the cycle, that is, the reversible capacities decrease gradually; for the same sample and same cycles, with the increase of the charge–discharge rate, the first two charge plateaus become smooth, which may be due to the rise of the electrode polarization. Although declined electrochemical performance is presented with the increase of the charge–discharge rate and cycle, 95.8 and 90 mAh g^{-1} capacities can still be kept under 10 C rate in the 300th cycle for the LVP1 and LVP2, respectively.

The cyclic performance of the LVP1/C and LVP2/C is evaluated in the cell configuration $Li/Li_3V_2(PO_4)_3$. As observed from Fig. 6, the two samples exhibit good cyclic ability. The discharge capacities of the LVP1/C are 103.9 and 83.1 mAh g^{-1} for the 1st and 600th cycles at 3 C rate, respectively, with the discharge capacity retention of 80%; for the LVP2/C, the capacities are 99.9 and 88.9 mAh g^{-1} in the 1st and 600th cycles at 3 C rate, respectively, only 11% loss. When the charge–discharge rate is increased to 10 C rate, the first discharge capacities are 99.8 and 95.9 mAh g^{-1} for the LVP1/C and LVP2/C, respectively, and 95.8 and 90 mAh g^{-1} are kept in the 300th cycle, so 96% and 94% retention is reached, respectively. Especially, it is a common phenomenon that the discharge capacities increase during several cycles for the two electrodes, maybe responsible for the activation of the electrodes. The largest discharge capacity of 108.1 mAh g^{-1} is delivered for the LVP1/C at 3 C rate. The excellent cyclic performance of the LVP1/C and LVP2/C may be related to the pure phases, small particles, large specific surface areas and residual carbon. However, it can be observed that in the case of the LVP2/C, the discharge capacities change greatly in the initial cycles at 10 C rate, that is, the capacities increase during the several cycles, decline sharply during following cycling, then rise again, and in the end, mostly constant capacity is sustained. It is possible that high electrochemical reaction resistance and contact resistance owing to the bad morphology exist in the LVP2/C and then large electrode polarization is produced under high charge–discharge rate. While the inherent structural characteristics of monoclinic LVP and the existence of surface carbon make good electrochemical-cycling stability in the subsequent cycles.

3.3.4. Impedance studies

It can be seen that the two samples have different electrochemical properties. Electrochemical impedance is a major part of internal resistance of a battery and small impedance is favorable for the extraction and reinsertion of Li^+ ions during the charge and discharge processes [10]. In order to further investigate the different electrochemical behavior of the LVP1 and LVP2 electrodes, the electrochemical impedance spectra (EIS) were measured at different states of the charge and are presented in Fig. 7. It is remarkable that similar EIS patterns are demonstrated and com-

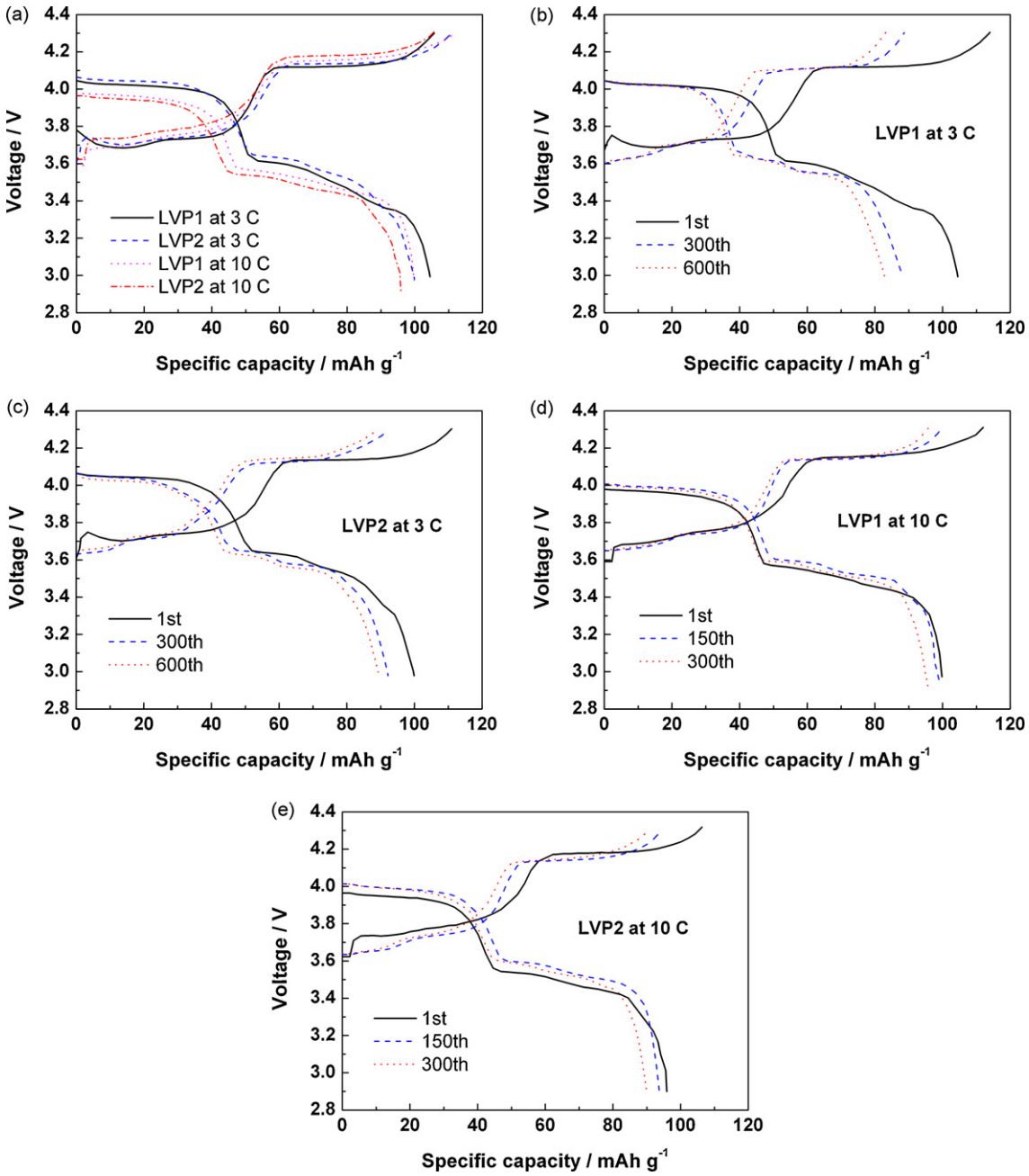

Fig. 5. (a) Initial charge–discharge profiles of LVP1/C and LVP2/C at different rates in the range of 3.0–4.3 V. (b)–(e) Voltage profiles of LVP1/C and LVP2/C in different cycles under 3 and 10 C rates.

posed of a small intercept in high frequency, a semicircle in high to medium frequency and a straight line in low frequency. Among, the small intercept is almost same for the two electrodes, about 6–9 Ω, which represents the solution resistance, that is, the resistance of the combination of the electrolyte and the electrode; the high frequency semicircle is assigned to the charge-transfer impedance in the electrode/electrolyte interface and the straight line is due to the diffusion of Li^+ ions in the electrode, i.e., the Warburg resistance. It is well known that it is important to have a small charge-transfer resistance for a cathode material with good electrochemical performance. As to the LVP/C, the diameter of the semicircle strongly relies on the potential during charging, that is, the charge-transfer resistance depends on the levels of the lithium extraction greatly. Lower charge-transfer resistance is got when higher potential is reached in Fig. 7. On the whole, low charge-transfer resistances are presented for the two electrodes, which possibly is ascribed to the small particles and the existence of the carbon. However, compared with the LVP2/C, the LVP1/C has even smaller charge-transfer resistance, which probably is attributed to a more uniform carbon network for the LVP1/C. This is good consistent with the SEM results.

In order to examine the extraction and reinsertion of the third Li^+ ion in the carbon-coated LVP composite materials, the charge–discharge tests in the range of 3.0–4.8 V were carried out, and the results are depicted in Fig. 8. It can be observed that the curves are similar in shapes. Four clear voltage plateaus are found on the charge curves at about 3.61, 3.69, 4.09 and 4.55 V, in which the plateau at 4.55 V is ascribed to the extraction of the third Li^+ ion, associated with the V^{4+}/V^{5+} redox couple. Besides, declining curves occur at the initial reinsertion of Li^+ ion, which represents the solid

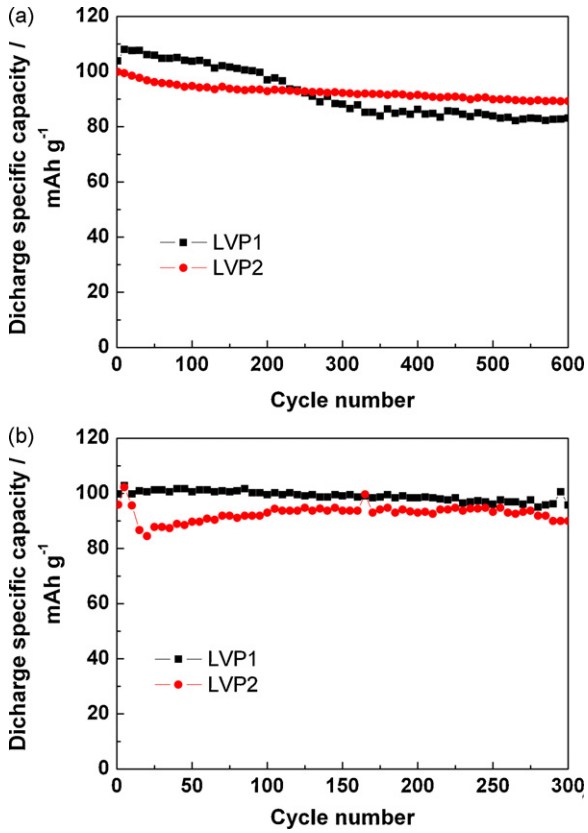

Fig. 6. Evolution of cycle capacity for LVP1/C and LVP2/C materials at (a) 3 C rate and (b) 10 C rate in the range of 3.0–4.3 V.

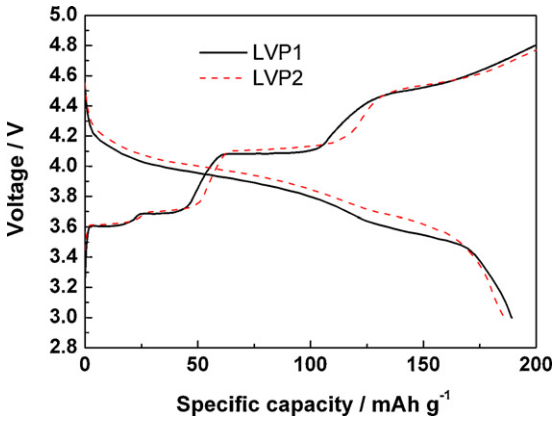

Fig. 8. Initial charge–discharge plots of LVP1/C and LVP2/C at 0.2 C rate in the range of 3.0–4.8 V.

solution behavior of Li^+ ion, and then the characteristic two-phase behavior reoccurs, corresponding to the reinsertion of the third Li^+ ion. In particular, 189.1 and 185.8 mAh g^{-1}, high initial reversible discharge capacities are reached at 0.2 C rate for the LVP1/C and LVP2/C, respectively. The capacities are larger than that of the LVP sample prepared by hydrogen reduction at 0.2 C rate [22]. It means that the electrochemical performance of the LVP has been greatly improved due to the coating of the carbon.

Additionally, the cyclic performance of the LVP1/C and LVP2/C composite materials was also evaluated at different current densities in the range of 3.0–4.8 V. As observed from Fig. 9, compared with the LVP2/C, higher discharge capacities are maintained for the LVP1/C electrode even at high rates. The initial discharge capacities of the LVP1/C are 184.2 and 165.3 mAh g^{-1} at 0.5 and 1 C

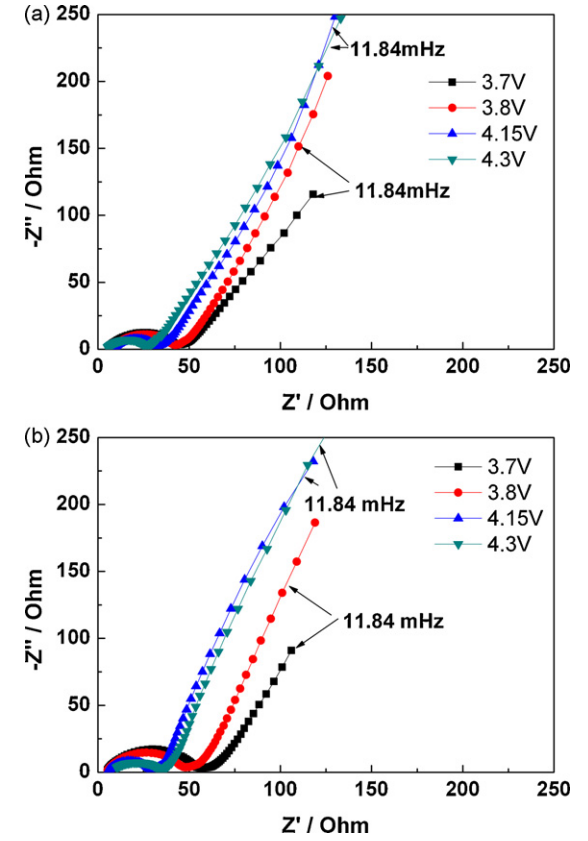

Fig. 7. Impedance spectra of (a) LVP1/C and (b) LVP2/C at different voltages during the first charging.

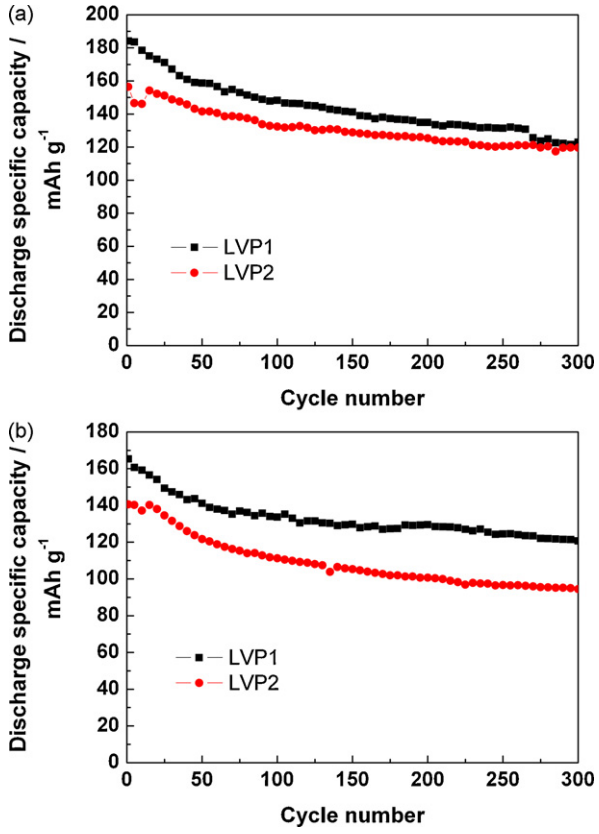

Fig. 9. Evolution of cycle capacity for LVP1/C and LVP2/C materials at (a) 0.5 C rate and (b) 1 C rate in the range of 3.0–4.8 V.

rates, respectively, and 158.7 (86.2% of initial discharge capacity) and 141.1 mAh g^{-1} (85.4% of initial discharge capacity) are preserved after 50 cycles. Moreover, discharge capacities of 123.0 and 120.7 mAh g^{-1} can still be sustained for the LVP1/C at 0.5 and 1 C after 300 cycles, respectively. In contrast, the LVP2/C has lower discharge capacities. When the rates are increased to 0.5 and 1 C rates, the discharge capacities are 156.4 and 140.6 mAh g^{-1} in the first cycle, and 119.6 and 94.5 mAh g^{-1} in the 300th cycle, respectively. The cyclic performance of the LVP1/C are better than that of the LVP2/C and are also comparable or even better than the earlier reports [9,14,19,26,32]. However, a rapid decay of the capacity on initial cycles is observed for the two electrodes, which may be due to the progressive dissolution of vanadium in the electrolyte and/or electrolyte decomposition and the increasing impedance at high voltage [1,8,11,16,33].

As we know, one of the factors for the capacity fading of cathode materials is the dissolution of the transition metal in electrolyte. Since the dissolution of the metals always appears at the interface between materials and electrolyte, a thin carbon layer could effectively prevent the dissolution of the vanadium from LVP [32]. Furthermore, the extraction of the third lithium ion occurs at about 4.55 V, a high voltage, at which it is easy to oxidize the electrolyte. And thus, uniform carbon layer on the LVP particles is of great use in keeping from the dissolution of the vanadium and the decomposition of the electrolyte. Compared with the LVP2, the particles of the LVP1 embedded in a uniform carbon network from the SEM result, which will be beneficial to its good electrochemical properties, especially when the cell is charged to 4.8 V, a high voltage.

4. Conclusions

The carbon-coated $Li_3V_2(PO_4)_3$ cathode materials have been successfully synthesized by a low temperature solid-state route using carbothermal reaction of vanadium with high valence. In addition, the influences of different heat treatments on the LVP electrodes have also been investigated. X-ray diffraction results show a pure single-phase with monoclinic structure for the two samples prepared by different heat treatments. From the SEM results, the LVP particles covered with carbon are about 0.5–1 μm in size. Most of the LVP1 particles are embedded in the carbon network, whereas the space of some LVP2 particles is large. The different micro-morphologies have influences on the electrochemical properties of the two samples. In the ranges of 3.0–4.3 V and 3.0–4.8 V, the initial discharge capacities of the LVP1/C electrode are larger than those of the LVP2/C electrode at different charge–discharge rates, which is due to a more uniform carbon coating for the LVP1 sample. In the range of 3.0–4.3 V, the two electrodes present fine reversibility, good rate capability and excellent cyclic performance with discharge capacities of 95.8 and 90 mAh g^{-1} after 300 cycles at 10 C for the LVP1/C and LVP2/C, respectively, which may be related to the existence of the carbon layer. While in the range of 3.0–4.8 V, the extraction the third Li^+ ion at about 4.55 V, and base on the high voltage the electrolyte is oxidized readily if the electrolyte and the LVP particles contact directly. However, since the improved homogeneity of the carbon dispersion for the LVP1/C, the initial discharge capacities of 189.1 and 165.3 mAh g^{-1} are delivered at 0.2 and 1 C rates in the range of 3.0–4.8 V, respectively, and 120.7 mAh g^{-1} is still sustained after 300 cycles at 1 C rate. For the LVP2/C electrode, poorer electrochemical properties are presented in the same range, which may be ascribed to its lower carbon coating status. In summary, based on the XRD results, the SEM images and the EIS studies of the two composite materials, the high capacity, good rate capability and excellent cyclic performance are owing to the small crystal grain originated from low calcination temperature and short sintering time, even particles, and the homogeneous carbon coating which improves the specific surface areas of the particles and enhances the electronic conductivity of the electrodes. However, it is apparent that the electrochemical performance of the two electrodes are poorer between 3.0 and 4.8 V than that in the range of 3.0–4.3 V. Thereby, efforts to improve the rate capability and cyclic performance of the LVP/C composite materials in the range of 3.0–4.8 V are underway in our laboratory.

References

[1] H. Huang, S.-C. Yin, T. Kerr, N. Taylor, L.F. Nazar, Adv. Mater. 14 (2002) 1525–1528.
[2] L.S. Cahill, R.P. Chapman, J.F. Britten, G.R. Goward, J. Phys. Chem. B 110 (2006) 7171–7177.
[3] D. Morgan, G. Ceder, M.Y. Saidi, J. Barker, J. Swoyer, H. Huang, G. Adamson, Chem. Mater. 14 (2002) 4684–4693.
[4] D. Morgan, G. Ceder, M.Y. Saidi, J. Barker, J. Swoyer, H. Huang, G. Adamson, J. Power Sources 119–121 (2003) 755–759.
[5] M.Y. Saidi, J. Barker, H. Huang, J.L. Swoyer, G. Adamson, Electrochem, Solid State Lett. 5 (2002) A149.
[6] S.-C. Yin, H. Grondey, P. Strobel, M. Anne, L.F. Nazar, J. Am. Chem. Soc. 125 (2003) 10402–10411.
[7] S.-C. Yin, H. Grondey, P. Strobel, H. Hunag, L.F. Nazar, J. Am. Chem. Soc. 125 (2003) 326–327.
[8] S. Patoux, C. Wurm, M. Morcrette, G. Rousse, C. Masquelier, J. Power Sources 119–121 (2003) 278–284.
[9] A.P. Tang, X.Y. Wang, S.Y. Yang, J.Q. Cao, J. Appl. Electrochem. 38 (2008) 1453–1457.
[10] C.X. Chang, J.F. Xiang, X.X. Shi, X.Y. Han, L.J. Yuan, J.T. Sun, Electrochim. Acta 53 (2008) 2232–2237.
[11] X.H. Rui, C. Li, C.H. Chen, Electrochim. Acta 54 (2009) 3374–3380.
[12] C.X. Chang, J.F. Xiang, X.X. Shi, X.Y. Han, L.G. Yuan, J.T. Sun, Electrochim. Acta 54 (2008) 623–627.
[13] X.J. Zhu, Y.X. Liu, L.M. Geng, L.B. Chen, J. Power Sources 184 (2008) 578–582.
[14] A.P. Tang, X.Y. Wang, Z.M. Liu, Mater. Lett. 62 (2008) 1646–1648.
[15] X.C. Zhou, Y.M. Liu, Y.L. Guo, Solid State Commun. 146 (2008) 261–264.
[16] Q.Q. Chen, J.M. Wang, Z. Tang, W.C. He, H.B. Shao, J.Q. Zhang, Electrochim. Acta 52 (2007) 5251–5257.
[17] Y.Z. Li, Z. Zhou, M.M. Ren, X.P. Gao, J. Yan, Electrochim. Acta 51 (2006) 6498–6502.
[18] Y.Z. Li, X. Liu, J. Yan, Electrochim. Acta 53 (2007) 474–479.
[19] M.M. Ren, Z. Zhou, Y.Z. Li, X.P. Gao, J. Yan, J. Power Sources 162 (2006) 1357–1362.
[20] M. Sato, H. Ohkawa, K. Yoshida, M. Saito, K. Uematsu, K. Toda, Solid State Ionics 135 (2000) 137–142.
[21] J. Barker, M.Y. Saidi, J.L. Swoyer, J. Electrochem. Soc. 150 (2003) A684–A688.
[22] M.Y. Saidi, J. Barker, H. Huang, J.L. Swoyer, G. Adamson, J. Power Sources 119–121 (2003) 266–272.
[23] P. Fu, Y.M. Zhao, Y.Z. Dong, X.N. An, G.P. Shen, Electrochim. Acta 52 (2006) 1003–1008.
[24] Y.Z. Li, Z. Zhen, X.P. Gao, J. Yan, Electrochim. Acta 52 (2007) 4922–4926.
[25] J.C. Zheng, X.H. Li, Z.X. Wang, H.J. Guo, Q.Y. Hu, W.J. Peng, J. Power Sources 189 (2009) 476–479.
[26] A.P. Tang, X.Y. Wang, S.Y. Yang, Mater. Lett. 62 (2008) 3676–3678.
[27] M.M. Ren, Z. Zhou, X.P. Gao, W.X. Peng, J.P. Wei, J. Phys. Chem. C 112 (2008) 5689–5693.
[28] X.C. Zhou, Y.M. Liu, Y.L. Guo, Electrochim. Acta 54 (2009) 2253–2258.
[29] H.C. Shin, W.I. Chob, H. Jang, J. Power Sources 159 (2006) 1383–1388.
[30] X.J. Zhu, Y.X. Liu, L.M. Geng, L.B. Chen, H.X. Liu, M.H. Cao, Solid State Ionics 179 (2008) 1679–1682.
[31] C.M. Burba, R. Frech, Solid State Ionics 177 (2007) 3445–3454.
[32] T. Jiang, C.Z. Wang, G. Chen, H. Chen, Y.J. Wei, X. Liu, Solid State Ionics 180 (2009) 708–714.
[33] J. Barker, R.K.B. Gover, P. Burns, A. Bryan, J. Electrochem. Soc. 154 (2007) A307–A313.